On the Network Planning of Wavelength Switched Optical Networks with P2MP Transceivers

Ruoxing Li, Qian Lv, and Zuqing Zhu, *Fellow, IEEE*

***Abstract*—Recently, to cope with the ever-growing traffic volumes and network services in the Internet, the coherent point-to-multipoint transceivers (P2MP-TRXs) enabled by digital subcarrier modulation (DSCM) technique have been developed and viewed as a promising replacement of conventional point-to-point transceivers (P2P-TRXs), especially for the metro-aggregation networks with hub-and-spoke traffic patterns. Nevertheless, the network planning of wavelength switched optical networks (WSONs) with P2MP-TRXs can be rather complex, as additional correlated constraints are introduced to model the routing and spectrum assignment (RSA), and thus the problem cannot be solved with existing algorithms in the literature. In this paper, we study the network planning of WSONs with P2MP-TRXs, which not only includes the aforementioned subproblem of correlated RSA, but also the placement of P2MP-TRXs in hub-leaf-based groups and the corresponding subcarrier (SC) assignments. We first formulate an integer linear programming (ILP) model to formally describe and exactly solve the network planning problem. Then, two polynomial-time heuristics, based on layered auxiliary graph (LAG) and conflict graph (CG), respectively, are proposed to find near-optimal solutions. Finally, we perform extensive simulations to evaluate the proposed algorithms, and the simulation results confirm their performance and effectiveness.**

***Index Terms*—Wavelength switched optical networks, Point-to-multipoint transceivers, Routing and spectrum assignment, Layered auxiliary graph, Spectrum fragmentation.**

I. Introduction

OVER the past decade, communication service providers (CSPs) have been facing the pressure to increase network capacity, improve network flexibility, and reduce network cost consistently, to adapt to the exponential growth of services and traffic volume in the Internet [1, 2]. Hence, fiber-optic networks, which are the only feasible underlying infrastructure of metro and core networks, have undergone dramatic changes for better adaptivity and higher cost-efficiency [3]. One notable example is the development of flexible-grid elastic optical networking (EON) [4–6], which has significantly improved the agility of the optical layer and made the data transmissions in it much more spectrum-efficient and cost-effective. However, as network services and traffic volume are expected to continue growing in the future [7–10], CSPs have to search for new optical networking technologies continuously, especially for reducing the cost per bit (CpB) of their networks [11].

While state-of-art coherent point-to-point transceivers (P2P-TRXs) continue to hold down the CpB of serving bandwidth-intensive unicast flows in core networks, deploying these P2P-TRXs in metro-aggregation networks could be less desirable for a few reasons [12]. Most importantly, the traffic demands in metro-aggregation networks exhibit a distinct pattern of hub-and-spoke (H&S), where a hub node needs to communicate with multiple leaf nodes simultaneously. Also, the capacities of these networks need to be overprovisioned to maintain low capital expenditures (CAPEX) while coping with both long-term growth and short-term fluctuations of traffic [13]. To adapt to such pattern, CSPs can deploy a large number of P2P-TRXs in pairs at hub and leaf nodes (as shown in Fig. 1(a)) [14]. Nevertheless, this not only entails sub-optimal utilization of capacities but also complicates network architecture and operation, which hinders further optimization of CAPEX and operating expenses (OPEX) and makes it unsustainable [15].

On the other hand, recent advances on point-to-multipoint transceivers (P2MP-TRXs) have provided a promising alternative to handle the H&S traffic more cost-efficiently [15, 16]. Enabled by digital subcarrier modulation (DSCM), a P2MP-TRX provides a finer spectrum assignment granularity by generating a set of low-speed Nyquist sub-carriers (SCs) to fulfill the bandwidth of a wavelength channel, and can maintain its complexity and cost similar to those of a conventional P2P-TRX operating at the same maximum line-rate [12].

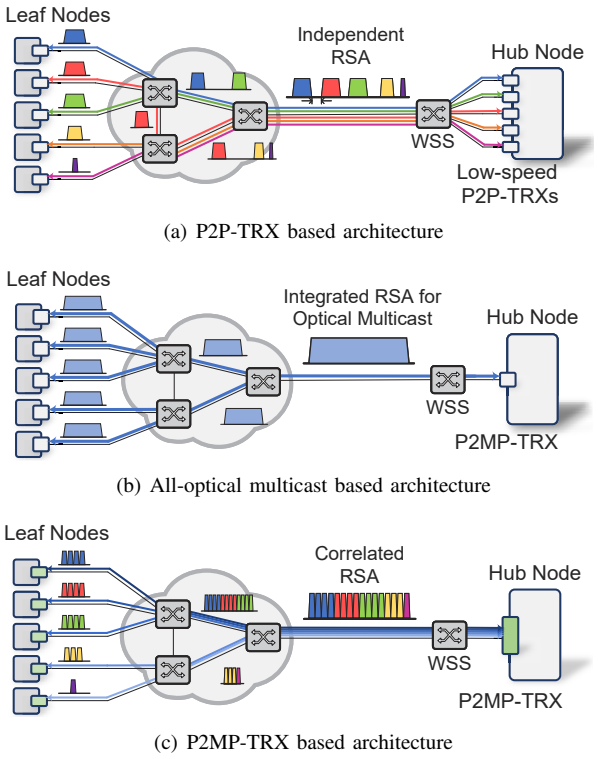

(a) P2P-TRX based architecture

(b) All-optical multicast based architecture

(c) P2MP-TRX based architecture

Fig. 1. Three network architectures to support H&S traffic in WSON.

R. Li, Q. Lv, and Z. Zhu are with the School of Information Science and Technology, University of Science and Technology of China, Hefei, Anhui 230027, P. R. China (email: zqzhu@ieee.org).

Manuscript received on October 11, 2022.

Despite their advantages, the planning of optical networks with P2MP-TRXs has just started to attract research interests [17–20]. However, existing studies on this topic all assumed a filterless optical network (FON) architecture [21], where a hub node talks with its leaf nodes with the "broadcast-and-select" scheme. While the structural compatibility of P2MP-TRXs and FON is good [18] and their symbiosis can indeed achieve appealing cost-effectiveness [19], the drawbacks of only considering P2MP-TRXs in FONs are also obvious. First, to avoid laser-loops, the filterless broadcast-and-select scheme can only be used in loopless fiber trees [22]. This, however, applies additional topology restrictions on the planned networks, *i.e.*, a planned network either can only use a tree-type topology [18, 20] or has to divide its physical topology into fiber trees [17, 19], which results in poor network reconfigurability. Second, an FON broadcasts the whole output of the P2MP-TRX at a hub node to all the nodes in its fiber tree. This leads to two levels of spectrum waste: 1) certain nodes on the fiber tree might not be leaf nodes of the hub node, and thus the spectra used on the fiber links to them are wasted, and 2) even for a leaf node, it does not need to receive the whole output of the P2MP-TRX as certain SCs might not be destined to it. Therefore, it is relevant to study how to plan wavelength switched optical networks (WSONs) with P2MP-TRXs, for better scalability, reconfigurability, and spectrum-efficiency.

Nevertheless, although the optical filtering techniques that can facilitate SC-level sub-wavelength switching have already been validated decades ago (*e.g.*, those based on fiber Bragg gratings (FBGs) [23, 24]) and P2MP-TRXs are backward compatible to fixed-/flexible-grid optical networks [25, 26], the network planning of WSONs with DSCM-based P2MP-TRXs, to the best of our knowledge, has not been studied in the literature yet. Specifically, such network planning starts with a physical topology to determine the allocation of P2MP-TRXs, assignment of SCs to P2MP-TRXs, and routing and spectrum assignment (RSA), for satisfying traffic demands. Due to the fundamental differences between FON and WSON, the existing approaches for planning P2MP-TRX-based FONs cannot be leveraged to solve this problem. For instance, due to the broadcast-and-select scheme, the RSA in P2MP-TRX-based FONs is simple or even trivial, but that in P2MP-TRX-based WSONs is rather complex, or even more complex than the conventional RSA in EONs, as we will explain below.

Fig. 1(a) gives an example to explain the RSA for planning lightpaths to carry H&S traffic in a WSON based on P2P-TRXs, which is actually similar to the basic case of RSA in EONs and can be solved with numerous existing algorithms. Note that, although all the lightpaths are from a same hub node, their RSA schemes are actually independent as long as the spectrum continuity, contiguity, and non-overlapping constraints [27] are satisfied by each of them. The example in Fig. 1(b) shows how to leverage all-optical multicast to carry H&S traffic in a P2MP-TRX-based WSON, where the basic idea is still "broadcast-and-select". Specifically, we first calculate a light-tree in the WSON, which covers the hub node and all of its leaf nodes, and then allocate sufficient spectrum on each link in the light-tree to accommodate the whole output of the P2MP-TRX at the hub node. The planning of the architecture in Fig. 1(b) can also be solved with the existing algorithms for multicast-capable RSA [28]. However, there is still spectrum waste on each light-tree, due to the lack of optical filtering on its branches. Note that, the common wavelength-selective switches (WSS') in a WSON cannot support all-optical multicast [29], while multicast-capable WSS' are usually much more complex and expensive [30].

In this work, we consider the architecture in Fig. 1(c) to plan P2MP-TRX-based WSONs. Specifically, each hub node and all of its leaf nodes are still covered by a light-tree, but the spectrum assignment on each branch of the light-tree is tailored to only deliver the required SCs of the leaf node that terminates the branch. Note that, as the SCs on all the branches are from the same P2MP-TRX, their spectrum usages are tightly correlated. In other words, the spectrum assignments on branches of the light-tree can only vary in a fixed spectral range. For instance, if we assume that a 400-Gbps P2MP-TRX uses the DSCM scheme with 16 SCs, each of which occupies 4 GHz[1] to achieve a capacity of 25 Gbps with dual-polarization and 16 quadrature amplitude modulation (DP-16QAM) [12], all the SCs from it have to be closely packed within 64 GHz. Obviously, such a correlated RSA for light-trees is much more complex than the RSA for the architectures in Figs. 1(a) and 1(b). To the best of our knowledge, the correlated RSA cannot be solved with any of the existing algorithms in the literature.

In this paper, we study the aforementioned network planning problem, which not only addresses the challenging subproblem of correlated RSA but also determines the allocation of P2MP-TRXs and assignment of SCs to P2MP-TRXs, such that the CAPEX of the planned P2MP-TRX-based WSON can be minimized. The usage of fiber links and the deployment of optical switches are also taken into consideration to further suppress expenditure waste due to overdesign. We first formulate an integer linear programming (ILP) model to formally describe the problem and solve it exactly. Then, to speed up the network planning, we propose two effective polynomial-time heuristics based on layered auxiliary graph (LAG) and conflict graph (CG), respectively, both of which can solve the correlated RSA for light-trees without introducing excessive spectrum fragmentation. Extensive simulations are carried out with three different topologies to evaluate our proposals in detail, and the simulation results confirm their performance and effectiveness.

The rest of this paper is organized as follows. Section II presents a brief review of the related works. In Section III, we describe the network model of P2MP-TRX-based WSONs and the network planning based on it. The ILP is formulated in Section IV, while the heuristics are designed in Section V. We discuss the simulations for performance evaluations in Section VI. Finally, Section VII summarizes the paper.

II. Related Work

DSCM has been regarded as a key technique to improve the agility of optical communications [31]. Specifically, DSCM uses Nyquist shaping to generate a set of closely packed,

[1]The bandwidth of 4 GHz for each SC is estimated after considering the real-world overheads such as forward error correction (FEC) overhead, signal roll-off factor, and spectrum guard-bands between SCs [25].

low-speed SCs (*e.g.*, at 4 GHz [12]) with a single laser, and thus the physical-layer impairments caused by fiber dispersion and nonlinearity can be effectively mitigated [32]. Hence, it enables longer-reach transmission with spectrally more efficient modulation formats [31], and can achieve notable energy-saving through autonomous SC configurations [25]. With DSCM-based P2MP-TRXs, the SCs generated by a hub node can be independently managed and destined to each of its leaf nodes, potentially providing the SC-level spectrum allocation granularity at a few GHz [20] (*i.e.*, even finer than that achieved by bandwidth-variable transponders in EONs).

The performance of P2MP-TRXs has been evaluated in both lab environments [33] and field trials [34], while the techno-economic comparisons of P2MP-TRXs and P2P-TRXs have been conducted in [15, 16]. Based on the FON architecture [22], there have been a few studies on the network planning and provisioning with P2MP-TRXs [17–20, 35]. The study in [18] tried to plan P2MP-TRX-based FONs with horseshoe topologies, but its optimization model did not address SC and spectrum assignments. The authors of [20] studied the survivable planning of FONs with P2MP-TRXs, by extending their seminar work in [17]. Specifically, they formulated an ILP model to set up spectrally-disjoint fiber-trees for link protection and leveraged sparse placement of red and blue filters to avoid laser-loops. As for multi-layer planning, Pavon-Marino *et al*. [19] investigated how to deploy P2MP-TRXs in fault-tolerant ring FONs under various traffic distributions, where a mixed ILP (MILP) model was formulated to overcome the sub-optimality of their previous proposal [35], and they also used wavelength blockers to avoid laser-loops.

However, none of the aforementioned studies on network planning has considered P2MP-TRX-based WSONs. As we have explained before, FON has drawbacks like spectrum waste and poor network reconfigurability [22]. Spectrum waste might not be welcome in the spectrum-starved regions where the cost of deploying new fibers is prohibitively high [36], and poor network reconfigurability makes it impractical to dynamically reconfigure the fiber-trees in an FON for adapting to dynamic traffic demands, because the reconfiguration needs to modify the fiber interconnections within FON nodes [22].

WSON can address the issues with FON by using wavelength or sub-wavelength switching, and thus P2MP-TRX-based WSONs can potentially achieve better scalability, reconfigurability, and spectrum-efficiency. Specifically, the two commonly-used optical switch architectures, which are route-and-select and broadcast-and-select [37], can be leveraged to realize SC-level sub-wavelength switching. As for the optical filtering elements in these switches, the SC-level sub-wavelength switching capability of FBG-based filters has been validated decades ago [23, 24], while the recent advances on liquid-crystal-on-silicon-based WSS' have also led to the commercial products that can facilitate SC-level sub-wavelength optical switching [38]. Note that, the optical switches based on broadcast-and-select may be more preferable for the deployment of P2MP-TRXs, thanks to its inherent capability to support all-optical multicast [29, 30], and thus the potential use cases of P2MP-TRXs in metro and core networks have just started to gain attentions [39, 40]. Hence, it is realistic and relevant to study the network planning of P2MP-TRX-based WSONs. Nevertheless, to the best of our knowledge, this problem has not been addressed in the literature yet.

III. Problem Description

In this section, we define the network model of P2MP-TRX-based WSONs and describe the network planning based on it.

We denote the physical topology as a graph $G(V, E)$, where V and E are the sets of nodes and fiber links, respectively. For each node $v \in V$, an optical switch can be deployed to realize sub-wavelength switching with the granularity of a frequency slot (FS), each of which has a bandwidth of 12.5 GHz, same as the common case in EONs [4] for backward compatibility.Meanwhile, to satisfy the pending traffic demands, each node v can be either a hub node, a leaf node, or both. We use O_h and O_l to respectively denote the sets of the types (in terms of capacities) of hub and leaf P2MP-TRXs. According to [12], O_h and O_l should partially intersect (*i.e.*, $O_h \cap O_l \neq \emptyset$), since certain P2MP-TRXs can be used on both hub and leaf nodes.

As we consider static network planning, we need to determine the placement of P2MP-TRXs on each node $v \in V$, and solve the correlated RSA for setting up lightpaths to interconnect the deployed P2MP-TRXs, such that all the pending traffic demands can be satisfied. Meanwhile, the usage of optical switches and fiber links should also be determined to avoid unnecessary expenditure. We model the pending traffic demands as a matrix $\mathbf{D} = [D_{u,v}]_{|V|\times|V|}$, where each element $D_{u,v}$ denotes the amount of traffic demand from u to v ($u, v \in V$), in terms of the number of SCs when each SC provides the lowest feasible capacity [20]. For convenience, we treat a hub P2MP-TRX and all of its leaf P2MP-TRXs as a group. Then, based on the traffic demands in $\mathbf{D}$, we can determine the capacities of the P2MP-TRXs in a group with an leader-follower approach. Specifically, the capacity of the hub P2MP-TRX is first selected (the leader) and then the capacity of each leaf P2MP-TRX is chosen accordingly (the follower). In order to clearly describe the relations among P2MP-TRXs hereinafter, we introduce the following definition.

Definition 1: We say *a P2MP-TRX m depends on another P2MP-TRX n*, if n and m are in the same group and n is designated as the hub P2MP-TRX of the group.

Each hub P2MP-TRX divides its capacity to assign to the P2MP-TRXs depending on it, in terms of non-overlapping SCs. The symbol rate B_s of each SC is fixed and predetermined by the hardware implementation of P2MP-TRXs. But as the SCs from a hub P2MP-TRX can actually be managed independently and thus assigned with different modulation formats [12], we let the hub P2MP-TRX choose the modulation format of the SCs assigned to each leaf P2MP-TRX based on the length of the lightpath between the hub-leaf pair [15]. Besides, although the duplex communications between a hub-leaf pair can be routed independently, for simplicity we assume that they are routed over the same path in both directions [25].

When assigning the SCs of a hub P2MP-TRX to its leaf P2MP-TRXs, we need to satisfy the SC contiguity constraint, *i.e.*, the SCs allocated to each leaf P2MP-TRX have to be contiguous in the spectrum domain. In this work, we assume

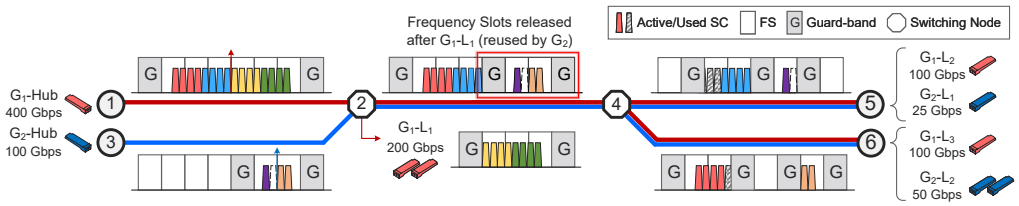

Fig. 2. Example on spectrum saving and reuse in P2MP-TRX-based WSONs.

that the bandwidth of each SC is 4 GHz. The spectra on each fiber link of a WSON are allocated to lightpaths in terms of FS', each of which can only be allocated to one group at most.

As explained in Fig. 1(c), a P2MP-TRX-based WSON can use optical filtering to ensure that each leaf P2MP-TRX only receives the SCs that are destined to it. Hence, unnecessary spectrum waste is avoided, which can be seen in the illustrative example in Fig. 2, where *Nodes* 2 and 3 are equipped with optical switches. Here, G_n denotes the n-th group, G_n-*Hub* is the hub P2MP-TRX of the n-th group, and G_n-L_m represents the m-th leaf P2MP-TRX in the n-th group. As shown in Fig. 2, after the SCs assigned to G_1-L_1 arriving and being received at *Node* 2, the WSON filters out the FS' accommodating these SCs. Here, only FS' that are no longer occupied by any active SCs can be released, and there are cases that SCs are already received but not completely filtered out in the subsequent links, e.g., the ones in *Links* 4-5 and 4-6. The released FS' can then be efficiently reused by the P2MP-TRX group G_2, with their leftmost FS serving as guard-band between G_1 and G_2.

IV. ILP Formulation

In this section, we formulate an ILP model for the network planning of a P2MP-TRX-based WSON and solve it exactly. Specifically, the ILP takes the physical topology, traffic matrix, and information about P2MP-TRXs as inputs, and aims to minimize the CAPEX of the planned WSON, including the costs of P2MP-TRXs and optical switches deployed on nodes, as well as those of the used fiber links and spectra usage. Tables I and II list the notations of the parameters and decision varables used in the ILP model, respectively.

Objective:

The objective is set as to minimize the normalized CAPEX of the planned WSON for provisioning all the demands in $\mathbf{D}$:

$$\text{Minimize} \quad \gamma_1 \cdot \frac{\mathcal{C}_T}{\hat{\mathcal{C}}_T} + \gamma_2 \cdot \frac{\mathcal{C}_F}{\hat{\mathcal{C}}_F} + \gamma_3 \cdot \frac{\mathcal{C}_X}{\hat{\mathcal{C}}_X} + \gamma_4 \cdot \frac{f_M}{\hat{f}_M}, \tag{1}$$

where $\mathcal{C}_T$ is the total cost of the deployed P2MP-TRXs as

$$\mathcal{C}_T = \sum_{u \in V} \sum_{n \in [1, N_t]} \sum_{o \in O_h \cup O_l} t^o_{u,n} \cdot C^T_o, \tag{2}$$

$\mathcal{C}_F$ is the total cost introduced by fiber link usage as

$$\mathcal{C}_F = \sum_{e \in E} C^F_e \cdot w^F_e, \tag{3}$$

$\mathcal{C}_X$ is the total deployment cost of optical switches as

$$\mathcal{C}_X = \sum_{u \in V} C^X \cdot w^X_u \tag{4}$$

TABLE I
Notations of Parameters

$G(V, E)$	the physical topology of the WSON.
B_f/B_s	the bandwidth per FS/SC at GHz.
N_f	the maximum number of FS' that each fiber link $e \in E$ can accommodate.
N_t	the maximum number of P2MP-TRXs that can be placed on each node $v \in V$.
N_g	the number of guard-band FS' between lightpaths.
O_h/O_l	the set of capacity types of hub/leaf P2MP-TRXs.
C^T_o	the investment cost of a type-o P2MP-TRX.
C^F_e	the cost introduced by the usage of a fiber link e.
C^X	the cost of deploying an optical switch.
S_o	the maximum number of SCs that a type-o P2MP-TRX can provide/utilize in total.
F_o	the maximum number of FS' that a type-o P2MP-TRX can occupy in total.
$P^V_{u,v}$	the set of candidate paths between nodes u and v.
P^E_e	the set of candidate paths that use link e.
M_p	the spectral efficiency of the highest feasible modulation format for path p, as a multiple of the bit-rate of the lowest available modulation format of P2MP-TRXs.
$D_{u,v}$	the traffic demand from u to v, as a multiple of the lowest feasible rate that can be provided by an SC.
D_u	the boolean indicator that equals 1 if there are any traffic demand(s) from/to node u, and 0 otherwise.
Q_s/Q_l	a sufficiently small/large positive real number.

and γ_1, γ_2, γ_3 and γ_4 are the adjustable weights for balancing the respective importance of the cost components. Here, f_M denotes the spectrum usage of the planned WSON[2]. $\hat{\mathcal{C}}_T$, $\hat{\mathcal{C}}_F$, $\hat{\mathcal{C}}_X$ and $\hat{f}_M$ are the pre-calculated worst-case values for the costs, respectively, which are introduced for normalization.

Constraints:

1) *Hub-Leaf P2MP-TRX Dependency Constraints:*

$$\sum_{o \in O_h \cup O_l} t^o_{u,n} \leq 1, \quad \forall u \in V,\ n \in [1, N_t]. \tag{5}$$

Eq. (5) ensures that each deployed P2MP-TRX is of one type.

$$\sum_{o \in O_h \cup O_l} t^o_{u,n+1} \leq \sum_{o \in O_h \cup O_l} t^o_{u,n}, \quad \forall u \in V, n \in [1, N_t - 1]. \tag{6}$$

Eq. (6) ensures that a higher-indexed P2MP-TRX on each node will not be activated before any lower-indexed ones.

$$\sum_{u \in V} \sum_{n=1}^{N_t} \sum_{p \in P^V_{u,v}} h^{u,n}_{v,m,p} \leq 1, \quad \forall v \in V,\ m \in [1, N_t]. \tag{7}$$

[2]Similar to famous studies on EON planning in [27, 41], we use the MIFS of the planned WSON to represent the overall spectrum usage, because the WSON generally needs to allocate FS' on all of its fiber links according to the MIFS to ensure network connectivity [27].

TABLE II
NOTATIONS OF VARIABLES

f_M	the maximum index of used FS' (MIFS).
$t^o_{u,n}$	the boolean variable that equals 1 if the n-th P2MP-TRX deployed on node u is of type-o, and 0 otherwise.
$h^{u,n}_{v,m,p}$	the boolean variable that equals 1 if the m-th P2MP-TRX on v depends on the n-th P2MP-TRX on u and p is the route path between them, and 0 otherwise.
$q_{u,n,e}$	the boolean variable that equals 1 if the path for the n-th P2MP-TRX on u uses link e, and 0 otherwise.
$r^{u,n}_{v,m,e}$	the boolean variable that equals 1 if the paths for the n-th P2MP-TRX on u and the m-th P2MP-TRX on v share a fiber link e, and 0 otherwise.
$r^{u,n}_{v,m}$	the boolean variable that equals 1 if the paths for the n-th P2MP-TRX on u and the m-th P2MP-TRX on v share any fiber link, and 0 otherwise.
b_u	the boolean variable that equals 1 if there are any light-path(s) passing node u, and 0 otherwise.
w^F_e	the boolean variable that equals 1 if a fiber link e is used by any deployed P2MP-TRX, and 0 otherwise.
w^X_u	the boolean variable that equals 1 if node u is deployed with an optical switch, and 0 otherwise.
$s_{v,m,p}$	the number of SCs allocated to the m-th P2MP-TRX on node v, for its lightpath along path p.
$a^{u,n}_{v,m}$	the boolean variable that equals 1 if the FS' used by the n-th P2MP-TRX on node u are lower than those used by the m-th P2MP-TRX on node v, and 0 otherwise.
$z^{u,n}_{v,m}/z^{*u,n}_{v,m}$	the start/end index of the SCs that the n-th P2MP-TRX on u allocates to the m-th P2MP-TRX on v.
$f_{u,n}/f^*_{u,n}$	the start/end index of the FS' allocated to the n-th P2MP-TRX on node u.
$g^{v_1,m_1}_{v_2,m_2}$	the boolean variable that equals 1 if the m_1-th P2MP-TRX on v_1 and the m_2-th P2MP-TRX on v_2 both depend on a same P2MP-TRX, and 0 otherwise.
$f^{u,n}_{v,m}$	the integer variable that equals $f_{u,n}$ if the m-th P2MP-TRX on node v depends on the n-th P2MP-TRX on node u, and 0 otherwise.

Eq. (7) ensures that each P2MP-TRX depends on at most one P2MP-TRX (*i.e.*, a hub P2MP-TRX does not depends on any).

$$\sum_{o\in O_h} t^o_{u,n} + \sum_{o\in O_l} t^o_{v,m} \geq 2\cdot \sum_{p\in P^V_{u,v}} h^{u,n}_{v,m,p}, \quad \forall u,v\in V,\ n,m\in[1,N_t]\,. \tag{8}$$

Eq. (8) ensures that the dependencies can only be established between two P2MP-TRXs of hub and leaf types, respectively.

$$q_{v,m,e} \geq h^{u,n}_{v,m,p}, \quad \forall u,v\in V,\ n,m\in[1,N_t]\,,\ e\in E,\ p\in P^E_e\cap P^V_{u,v}, \tag{9}$$

$$Q_s\cdot\sum_{e\in E} r^{v_1,m_1}_{v_2,m_2,e} \leq r^{v_1,m_1}_{v_2,m_2} \leq \sum_{e\in E} r^{v_1,m_1}_{v_2,m_2,e}, \quad \forall v_1,v_2\in V, m_1,m_2\in[1,N_t]\,. \tag{10}$$

Eqs. (9) and (10) ensure that the fiber link(s) used and shared by the lightpaths of P2MP-TRXs are identified correctly.

2) *Optical Switch Deployment and Fiber Usage Constraints:*

$$Q_s\cdot\sum_{v\in V}\sum_{m=1}^{N_t} q_{v,m,e} \leq w^F_e \leq \sum_{v\in V}\sum_{m=1}^{N_t} q_{v,m,e}, \quad \forall e\in E. \tag{11}$$

Eq. (11) ensures that fiber link usages are determined correctly.

$$\sum_{e\in I_E(u)} q_{v,m,e} - 1 \leq b_u, \quad \forall u,v\in V, m\in[1,N_t]. \tag{12}$$

$$Q_l\cdot w^X_u \geq \sum_{e\in I_E(u)} w^F_e + D_u + b_u - 3, \quad \forall u\in V. \tag{13}$$

Eqs. (12) and (13) ensure that the deployment of optical switches is obtained correctly based on established lightpaths, where $I_E(u)$ denotes the neighboring links of a node u in G.

3) *P2MP-TRX Capacity Constraints:*

$$\begin{cases} s_{v,m,p} \leq \sum_{o\in O_l} t^o_{v,m}\cdot S_o, \\ s_{v,m,p} \leq Q_l\cdot\sum_{n=1}^{N_t} h^{u,n}_{v,m,p}, \end{cases} \quad \forall u,\ v,\ m,\ p\in P^V_{u,v}. \tag{14}$$

Eq. (14) ensures that SCs are assigned to P2MP-TRXs according to their dependencies, and do not exceed their capacities.

$$D_{u,v} \leq \sum_{n=1}^{N_t}\sum_{m=1}^{N_t}\sum_{p\in P^V_{u,v}} M_p\cdot(s_{v,m,p}+s_{u,n,p}), \quad \forall u,v\in V. \tag{15}$$

Eq. (15) ensures that each deployed P2MP-TRX has enough capacity to accommodate the traffic demands assigned to it.

4) *SC Assignment Constraints:*

$$\begin{cases} z^{u,n}_{v,m}, z^{*u,n}_{v,m} \in \left[\sum_{p\in P^V_{u,v}} h^{u,n}_{v,m,p},\ Q_l\cdot\sum_{p\in P^V_{u,v}} h^{u,n}_{v,m,p}\right], \\ z^{u,n}_{v,m}, z^{*u,n}_{v,m} \in \left[\sum_{o\in O_h} t^o_{u,n},\ S_o\cdot\sum_{o\in O_h} t^o_{u,n}\right], \end{cases} \quad \forall u,v\in V,\ n,m\in[1,N_t]\,. \tag{16}$$

Eq. (16) ensures that each hub P2MP-TRX can only allocate its SCs to its leaf P2MP-TRXs.

$$\sum_{n=1}^{N_t}\left(z^{*u,n}_{v,m} - z^{u,n}_{v,m}\right) + 1 \geq \sum_{p\in P^V_{u,v}} s_{v,m,p}, \quad \forall u,\ v,\ m. \tag{17}$$

Eq. (17) ensures that each leaf P2MP-TRX is allocated with enough SCs from its hub P2MP-TRX.

$$a^{v_1,m_1}_{v_2,m_2} + a^{v_2,m_2}_{v_1,m_1} = 1, \quad \forall v_1,v_2\in V,\ m_1,m_2\in[1,N_t]\,, \tag{18}$$

$$z^{*u,n}_{v_2,m_2} - z^{u,n}_{v_1,m_1} + 1 \leq Q_l\cdot\left[2 + a^{v_1,m_1}_{v_2,m_2} - \sum_p\left(h^{u,n}_{v_1,m_1,p} + h^{u,n}_{v_2,m_2,p}\right)\right], \quad \forall u,v_1,v_2\in V,\ n,m_1,m_2\in[1,N_t]\,. \tag{19}$$

Eqs. (18) and (19) ensure that the SCs assigned to different leaf P2MP-TRXs of a hub P2MP-TRX do not overlap.

5) *FS Assignment Constraints:*

$$f_{v,m}, f^*_{v,m}\in[1,N_f]\,, \quad \forall v\in V,\ m\in[1,N_t]\,. \tag{20}$$

Eq. (20) ensures that the FS' assigned to P2MP-TRXs are within the range defined by the capacity of each fiber link.

$$\begin{cases} f_{v,m} \leq N_f\cdot\sum_{o\in O_h} t^o_{v,m} + \sum_{u\in V}\sum_{n=1}^{N_t}\left[f^{u,n}_{v,m} + \frac{z^{u,n}_{v,m}\cdot B_s}{B_f} + \sum_{o\in O_h}\frac{F_o\cdot B_f - (S_o+2)\cdot B_s + Q_s}{2\cdot B_f}\cdot t^o_{u,n}\right], \\ f^*_{v,m} \geq \sum_{u\in V}\sum_{n=1}^{N_t}\left[f^{u,n}_{v,m} + \frac{z^{*u,n}_{v,m}\cdot B_s}{B_f} + \sum_{o\in O_h}\frac{F_o\cdot B_f - S_o\cdot B_s - Q_s}{2\cdot B_f}\cdot t^o_{u,n}\right], \end{cases} \quad \forall v\in V,\ m\in[1,N_t]\,. \tag{21}$$

Eq. (21) ensures that enough FS' are allocated to each P2MP-TRXs according to its dependency and allocated SCs.

$$f^*_{v_2,m_2} - f_{v_1,m_1} + N_g + 1 \leq N_f \cdot (1 + a^{v_1,m_1}_{v_2,m_2} - r^{v_1,m_1}_{v_2,m_2} + g^{v_1,m_1}_{v_2,m_2}), \quad \forall v_1, v_2 \in V,\ m_1, m_2 \in [1, N_t]\,. \tag{22}$$

Eq. (22), together with Eq. (18), ensures that the FS' allocated to P2MP-TRXs whose lightpaths share link(s) do not overlap.

$$f_M \geq f^*_{u,n}, \quad \forall u \in V,\ n \in [1, N_t]\,. \tag{23}$$

Eq. (23) determines the MIFS in the planned WSON.

6) *Linearization-related Constraints:*

$$\begin{cases} g^{v_1,m_1}_{v_2,m_2} \leq \sum\limits_{u' \in V} \sum\limits_{n'=1}^{N_t} \sum\limits_{p \in P^V_{u',v_1}} h^{u',n'}_{v_1,m_1,p}, \\ g^{v_1,m_1}_{v_2,m_2} \leq \sum\limits_{u' \in V} \sum\limits_{n'=1}^{N_t} \sum\limits_{p \in P^V_{u',v_2}} h^{u',n'}_{v_2,m_2,p}, \\ g^{v_1,m_1}_{v_2,m_2} \geq \sum\limits_{p} \left(h^{u,n}_{v_1,m_1,p} + h^{u,n}_{v_2,m_2,p} \right) - 1, \end{cases} \quad \forall u, v_1, v_2 \in V,\ n, m_1, m_2 \in [1, N_t]\,, \tag{24}$$

$$\begin{cases} f^{u,n}_{v,m} \leq f_{u,n}, \\ f^{u,n}_{v,m} \geq f_{u,n} + N_f \cdot \left(\sum\limits_{p \in P^V_{u,v}} h^{u,n}_{v,m,p} - 1 \right), \\ \sum\limits_{p \in P^V_{u,v}} h^{u,n}_{v,m,p} \leq f^{u,n}_{v,m} \leq N_f \cdot \sum\limits_{p \in P^V_{u,v}} h^{u,n}_{v,m,p}\,, \end{cases} \quad \forall u, v \in V,\ n, m \in [1, N_t]\,, \tag{25}$$

$$\begin{cases} r^{v_1,m_1}_{v_2,m_2,e} \leq q_{v_1,m_1,e}, \\ r^{v_1,m_1}_{v_2,m_2,e} \leq q_{v_2,m_2,e}, \\ r^{v_1,m_1}_{v_2,m_2,e} \geq q_{v_1,m_1,e} + q_{v_2,m_2,e} - 1, \end{cases} \quad \forall v_1, v_2 \in V, m_1, m_2 \in [1, N_t], e \in E. \tag{26}$$

Eqs. (24)-(26) are the linearization constraints for $g^{v_1,m_1}_{v_2,m_2}$, $f^{u,n}_{v,m}$, and $r^{v_1,m_1}_{v_2,m_2,e}$, respectively.

V. Heuristic Algorithms

The aforementioned ILP would be intractable for large-scale problems due to poor scalability. In this section, we design two heuristics to solve the network planning in polynomial time.

A. LAG-based Fragmentation-aware Network Planning

The planning of P2MP-TRX-based WSONs needs to allocate P2MP-TRXs in hub-leaf groups and determine the related SC assignments and RSA schemes with a leader-follower approach. Specifically, each hub-leaf group covers a light-tree, but the spectrum assignment on each of its branch can be different (*i.e.*, each leaf P2MP-TRX only needs to receive the SCs assigned to it). However, such correlated RSA in tree structures can fragment the spectra on fiber links severely if without proper SC and FS assignment strategies. This motivates us to 1) leverage the layered auxiliary graph (LAG) technique [42, 43] to calculate light-trees, and 2) design spectral and spatial fragmentation metrics specifically for P2MP-TRX-based planning to assist the SC assignments of leaf P2MP-TRXs, so as to improve the continuity and contiguity of available FS' on and between fiber links.

Algorithm 1: LAG-FA Network Planning

Input: Physical topology $G(V, E)$, traffic demands $\mathbf{D}$.
Output: Overall network planning scheme $\mathbb{Y}$.

while *there are non-zero element(s) in* $\mathbf{D}$ **do**
  select hub node v that maximizes $\sum_{u \in V} D_{v,u}$;
  for *each* $k \in [1, 1 + N_f - \hat{F}_o)]$ **do**
    get the k-th LAG $G_k(V_k, E_k)$ based on current network status, and set $X_k = \emptyset$;
    calculate a light-tree $\mathcal{T}_k$ in G_k to cover hub node v and nodes in $V' := \{u : D_{v,u} > 0, u \in V\}$;
    choose a proper P2MP-TRX $o_h \in O_h$ for hub v;
    for *each potential leaf node* $u \in V'$ **do**
      obtain the set of candidate P2MP-TRXs on u and insert them in set X_k;
    end
    $Y_k = \emptyset$, $j = 1$;
    while $X_k \neq \emptyset$ *AND* $j \leq S_{o_h}$ **do**
      calculate cut $c_{l,j}$ for each P2MP-TRX $x_l \in X_k$ at the j-th SC with Eq. (27);
      if *there exists a unique P2MP-TRX* x^*_l *whose cut is the smallest* **then**
        insert SC assignment $\{x^*_l, j, s_{x^*_l}\}$ in Y_k;
      else
        get misalignment $m_{l,j}$ for P2MP-TRXs whose cuts are the smallest, with Eq. (28);
        select P2MP-TRX x^*_l with the smallest misalignment, insert $\{x^*_l, j, s_{x^*_l}\}$ in Y_k;
      end
      remove x^*_l from X_k, and set $j = j + s_{x^*_l}$;
    end
    get the number of SCs used on hub P2MP-TRX o_h (namely, Z_k) according to Y_k;
    if $Z_k > Z_{k_0}$ **then**
      $k_0 = k$;
    end
  end
  insert Y_{k_0} in $\mathbb{Y}$ as provisioning scheme of current group led by a hub P2MP-TRX on node v;
  update $G(V, E)$ and $\mathbf{D}$ according to Y_{k_0};
end
Determine the deployment of optical switches and the activation of fiber links according to $\mathbb{Y}$;

Algorithm 1 shows our LAG-based fragmentation aware (LAG-FA) network planning, which uses a while-loop to serve all the traffic demands in $\mathbf{D}$ progressively. Here, we first assume that all the fiber links can be used by P2MP-TRXs when deploying them, and then activate fiber links based on their actual usage. This is because the leasing prices of fiber links are typically less expensive than the costs of P2MP-TRXs and optical switches [44]. Then, adequate network connectivity and flexibility can be ensured during service provisioning, which also improves the efficiency of spectrum utilization

through load-balancing [6]. In each iteration, we first find the node v whose pending out-going traffic amount is the largest, select it to place the next hub P2MP-TRX (*Line* 2). Then, the for-loop of *Lines* 3-25 tries to plan the WSON for the group led by the hub P2MP-TRX at node v based on LAGs. Note that, the "$\hat{F}_o$" in *Line* 3 is defined as $\hat{F}_o = \max_{o \in O_h}(F_o)$, *i.e.*, the maximum number of FS' that any type of hub P2MP-TRX can occupy. *Line* 4 builds the k-th LAG (*i.e.*, for the FS block (FSB) of $[k, k+\hat{F}_o-1]$), and initializes X_k. As shown in Fig. 3, each LAG only cares the availability of a block of $\hat{F}_o$ FS' on each link in $G(V, E)$. For instance, to build the first LAG G_1, we only add a link $e \in E$ in G_1 if the FSB of $[1, \hat{F}_o]$ on it is available. We then calculate a light-tree $\mathcal{T}_k$ in G_k, which tries to cover the hub node v and its potential leaf nodes in V' (*i.e.*, all the nodes that need to receive traffic from v).

Next, based on the light-tree $\mathcal{T}_k$ and pending traffic from v, we choose a proper hub P2MP-TRX type o_h from O_h for being placed on v (*Line* 6). Specifically, if the pending traffic amount from v exceeds the capacity of any P2MP-TRX type in O_h, we select the P2MP-TRX type whose capacity is the largest, and the one whose capacity is just enough otherwise. The for-loop of *Lines* 7-9 checks each potential leaf node $u \in V'$ to get its set of candidate P2MP-TRXs for receiving the traffic demand $D_{v,u}$, such that the number of candidate P2MP-TRXs is minimized. Then, all the candidate P2MP-TRXs are stored in set X_k. *Line* 10 is for the initialization of SC assignments[3].

The while-loop of *Lines* 11-20 leverages the fragmentation-aware (FA) approach in [6] to assign SCs to leaf P2MP-TRXs. Specifically, we extend the FA approach in [6] to evaluate the SC assignments to leaf P2MP-TRXs in both the spectral and spatial domains. We start with setting the start SC index as $j = 1$, and terminates the while-loop until all the candidate P2MP-TRXs in X_k have been taken care of or all the SCs of the hub P2MP-TRX have been checked (*i.e.*, $j > S_{o_h}$). For the SC assignment to a leaf P2MP-TRX $x_l \in X_k$ with start SC index j, we define the spectrum cut $c_{l,j}$ caused by it as

$$c_{l,j} = \begin{cases} 2 \cdot \vee\left[\delta_l^k \oplus \Delta(\beta_j^k)\right] - |p_l^k|, & \vee[\Delta(\beta_j^k)] \neq |\mathcal{T}_k|, \\ 2 \cdot \vee\left[\delta_l^k \oplus \Delta(\beta_j^k - 1)\right] - |p_l^k|, & \text{otherwise}, \end{cases} \tag{27}$$

where δ_l^k is a $|\mathcal{T}_k|$-bit mask indicating the fiber link usage when deploying P2MP-TRX $x_l \in X_k$ in the obtained light-tree $\mathcal{T}_k$ of the k-th LAG G_k, β_j^k denotes the starting index of FS' related to the assignment of the j-th SC in G_k, $\Delta(i)$ returns an $|\mathcal{T}_k|$-bit mask to denote the availability of the i-th FS on links in $\mathcal{T}_k$, $\vee[\cdot]$ returns the number of bit 1 in a bit-mask, p_l^k is the path used by P2MP-TRX x_l in G_k, and $|p_l^k|$ and $|\mathcal{T}_k|$ return the number of links in them.

For the same SC assignment, we also define the spectrum misalignment $m_{l,j}$ caused by it as

$$m_{l,j} = \sum_{e \in p_l^k, e' \in I_E(e) \setminus p_l^k} \left(2 \vee [\Theta_e^k \odot \Theta_{e'}^k \oplus \theta_{l,j}] - \vee[\theta_{l,j}]\right), \tag{28}$$

where $I_E(e)$ denotes the neighbor links of a link e in G_k, $\theta_{l,j}$ is a $\hat{F}_o$-bit mask indicating the FS' used by P2MP-TRX $x_l \in X_k$ in G_k, and Θ_e^k is also a $\hat{F}_o$-bit mask that tells the availability of FS' on link e in G_k. Therefore, we first calculate the cut caused by each candidate leaf P2MP-TRX $x_l \in X_k$ (*Line* 12). If there exists a unique P2MP-TRX x_l^* whose cut is the smallest, we just insert the P2MP-TRX and its SC assignment in set Y_k (*Lines* 13-14). Otherwise, we check the misalignments caused by the P2MP-TRXs whose cuts are the smallest, and insert the one with the smallest misalignment and its SC assignment in Y_k (*Lines* 15-17). Next, *Line* 19 removes the selected P2MP-TRX x_l^* from set X_k, and proceeds to the next available block of SCs from the hub P2MP-TRX.

In *Line* 21, we get the number of SCs used on the hub P2MP-TRX by the SC assignments in Y_k, and store it in Z_k. Then, *Lines* 22-24 select the optimal set of SC assignments Y_{k_0}, *i.e.*, the one that achieves the largest utilization of the SCs from the hub P2MP-TRX. After that, we insert Y_{k_0} in $\mathbb{Y}$ as the provisioning scheme of the current group led by the hub P2MP-TRX on node v, and update the network status for subsequent network planning (*Lines* 26-27). Finally, the usages of optical switches and fiber links are determined according to the deployed P2MP-TRXs and their lightpaths (*Line* 29).

Fig. 3 gives an example to explain the key steps of LAG-FA. Here, we have the group as $\{\text{hub}, x_1, x_2, x_3\}$, whose P2MP-TRX locations are shown in Fig. 3(a). The right subplot of Fig. 3(a) is for the spectrum usage in the WSON before serving the group, where the gray blocks are for the FS' that have already been used. Fig. 3(b) shows the first two LAGs obtained for serving the group, and it can be seen that only in the second

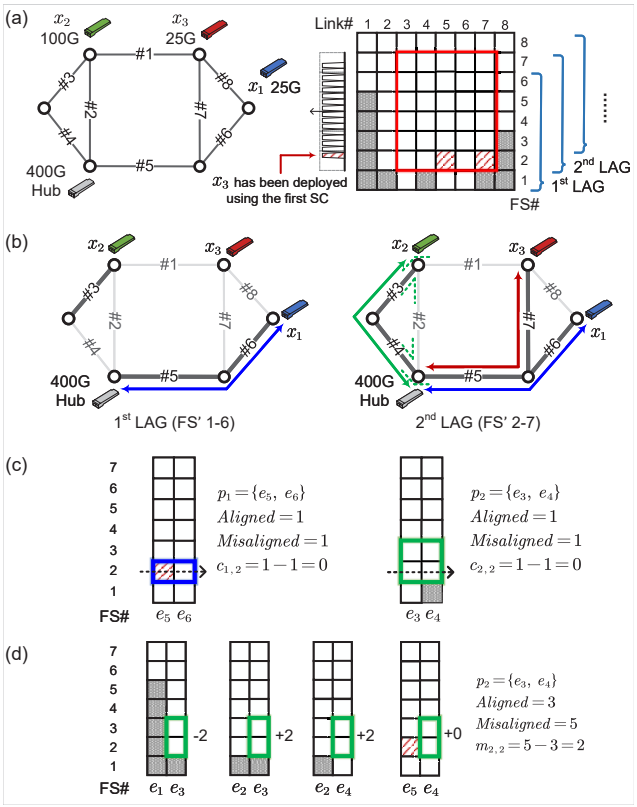

Fig. 3. An example on LAG-FA, a) Physical topology and spectrum usage, b) LAGs obtained for serving the group of $\{\text{hub}, x_1, x_2, x_3\}$, (c) Cuts induced by the SC assignments to x_1 and x_2 with start SC index $j = 2$, d) Misalignment induced by the SC assignment to x_2 with start SC index $j = 2$.

[3]With the bandwidths of each SC and each FS, we can easily map the SC assignments in each LAG to FS assignments.

LAG, a feasible light-tree can be obtained to interconnect the hub P2MP-TRX and all of its leaf P2MP-TRXs. Here, we assume that the SC assignment of leaf P2MP-TRX x_3 has already determined to use start SC index $j = 1$. Hence, the FS usage of x_3 is also plotted in the right subplot of Fig. 3(a) with red-slashed blocks. As the first SC from the hub P2MP-TRX has been assigned to x_3, the SC assignments to x_1 and x_2 can only start with SC index $j = 2$, and their spectrum cuts with Eq. (27) are shown in Fig. 3(c). Since the cuts of the two SC assignments are the same, LAG-FA proceeds to check their misalignments with Eq. (28). As illustrated in Fig. 3(d), the misalignment of the SC assignment of x_2 is $m_{2,2} = 2$. Similarly, we can obtain $m_{1,2} = -5$. Finally, LAG-FA assigns x_1, x_2, and x_3 to use *SC* 2, *SCs* 3-6, and *SC* 1, respectively.

Complexity Analysis: In the worst case, the outer while-loop can be executed $\mathcal{D}$ times, where $\mathcal{D} = \sum_{u,v \in V} D_{u,v}$. The for-loop of *Lines* 3-29 can run for $O(N_f)$ times, while the time complexity of getting an LAG is $O(|E|)$. As for the light-tree calculation, the complexity is $O(|E| + |V| \cdot \log |V|)$ [45] and $O(\hat{S}_o \cdot |V|^2)$ [46], if we use the shortest path tree (SPT) and minimum spanning tree (MST) algorithms, respectively, where $\hat{S}_o$ denotes the maximum number of SCs that any type of P2MP-TRX in $O_h \cup O_l$ can use. Hence, the overall complexity of *Algorithm* 1 is $O(N_f \cdot (\mathcal{D} + |O_h|) \cdot (\hat{S}_o \cdot |V| \cdot \log(\hat{S}_o \cdot |V|) + \hat{S}_o^3 \cdot |E|^2))$ if SPT is used, and $O(N_f \cdot (\mathcal{D} + |O_h|) \cdot (\hat{S}_o \cdot |V|^2 + \hat{S}_o \cdot |V| \cdot \log(\hat{S}_o \cdot |V|) + \hat{S}_o^3 \cdot |E|^2))$ if MST is applied.

B. CG-MWIS-based Network Planning

The LAG-FA algorithm can address spectrum fragmentation during network planning. However, as each LAG is built based on the availability of a whole FSB of $\hat{F}_o$ FS' on each link, the SC/FS assignments based on it are still too coarse-grained to resolve spectrum fragmentation effectively. Hence, we propose another heuristic that can realize finer-grained scanning for available SCs during network planning.

We still check the spectrum availability in $G(V, E)$ based on FSBs. Specifically, each FSB includes $\hat{F}_o$ FS', and the k-th FSB covers the FS' $[k, k + \hat{F}_o - 1]$ on each link $e \in E$. Then, when attempting to deploy a group of P2MP-TRXs with an FSB, we first find all the available SCs on all the links based on their spectrum usages in the FSB, and then compute a light-tree accordingly for establishing connections for the P2MP-TRX group. Next, the goal is to utilize the fragmented spectra on the light-tree to serve as many traffic demands of the group as possible. Nevertheless, in order to achieve the goal, we need to resolve the conflicts among the SC assignments of candidate leaf P2MP-TRXs. To this end, we formulate the following ILP to describe the problem of leaf P2MP-TRX deployment and SC assignment with the k-th FSB in $G(V, E)$.

Parameters:

- X_k: the set of the candidate leaf P2MP-TRXs that can be deployed with the k-th FSB for the current group.
- $J_{k,n}$: the set of start SC indices with which the n-th candidate leaf P2MP-TRX in X_k can be deployed.
- $W_{k,n}$: the traffic demand that can be provisioned by the n-th candidate leaf P2MP-TRX in X_k.
- $C_{k,n}$: the cost introduced by deploying the n-th candidate leaf P2MP-TRX in X_k.
- $U_{n,j}^{m,i}$: the boolean indicator that equals 1 if the deployment of the n-th candidate leaf P2MP-TRX with j as start SC index conflicts with that of the m-th candidate leaf P2MP-TRX with i as start SC index, and 0 otherwise.

Variables:

- $x_{n,j}^k$: the boolean variable that equals 1 if the n-th candidate leaf P2MP-TRX in X_k is deployed and j is the start SC index of its SC assignment, and 0 otherwise.

Objective:

The optimization objective is set to first maximize the traffic demands served by the current P2MP-TRX group and then minimize the total cost of the deployed P2MP-TRXs.

$$\text{Maximize} \sum_{n \in [1, |X_k|],\ j \in J_{k,n}} (W_{k,n} - Q_s \cdot C_{k,n}) \cdot x_{n,j}^k. \quad (29)$$

Constraint:

$$x_{n,j}^k + x_{m,i}^k + U_{n,j}^{m,i} \leq 2, \quad \forall n, m \in [1, |X_k|], j \in J_{k,n}, i \in J_{k,m}. \quad (30)$$

Eq. (30) ensures that the SC assignments of two candidate leaf P2MP-TRXs cannot be chosen simultaneously if there are conflict(s) between them. More specifically, there can be two types of conflicts between the SC assignments: 1) the feasible SC assignments of a same candidate leaf P2MP-TRX conflict with each other, and 2) the feasible SC assignments of two different candidate leaf P2MP-TRXs have conflicts between each other if they have spectrum conflict(s).

The optimization in the ILP above can be better modeled by leveraging a conflict graph (CG) $G^C(V^C, E^C)$. Specifically, we denote each feasible SC assignment of a candidate leaf P2MP-TRX (*i.e.*, $x_{n,j}^k$) as one node in V^C, whose weight is set as the traffic demand that can be served by this P2MP-TRX (*i.e.*, $W_{k,n}$) minus a small penalty related to the P2MP-TRX's cost (*i.e.*, $Q_s \cdot C_{k,n}$). Two nodes are connected with a link in E^C if there are aforementioned conflicts between the feasible SC assignments represented by them. Therefore, the original optimization gets transformed into finding the maximum-weighted independent set (MWIS) in the CG. Although the problem of finding MWIS in an arbitrary graph is $\mathcal{NP}$-hard, we can leverage existing approaches in the literature to solve it in polynomial time with reasonably good approximation ratio (*e.g.*, the distributed greedy (DistGreedy) algorithm in [47]).

Fig. 4 explains how to utilize a CG to model and solve the SC assignment problem for candidate leaf P2MP-TRXs. The physical topology, spectrum usage, and light-tree for the group $\{\text{hub}, x_1, x_2, x_3, x_4\}$ are shown in Fig. 4(a). Based on the spectrum usage, we obtain all the possible SC assignments for candidate leaf P2MP-TRXs, as plotted in Fig. 4(b). Here, we just use the possible SC assignments of x_2 and x_4 to explain the two types of conflicts in the CG: 1) the conflicts between SC assignments of a same P2MP-TRX, and 2) the spectral conflicts between SC assignments of different P2MP-TRXs. Finally, an MWIS can be obtained in the CG, which is denoted with the red nodes in Fig. 4(b) (*i.e.*, $\{x_{1,4}, x_{2,13}, x_{3,3}, x_{4,1}\}$) and indicates the SC assignments of the leaf P2MP-TRXs.

Algorithm 2 explains the details of the CG-MWIS-based network planning, which generally follows a similar procedure

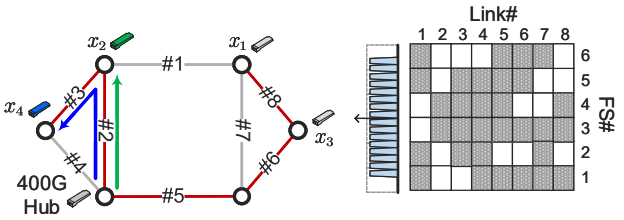

(a) Physical topology, spectrum usage, and light-tree.

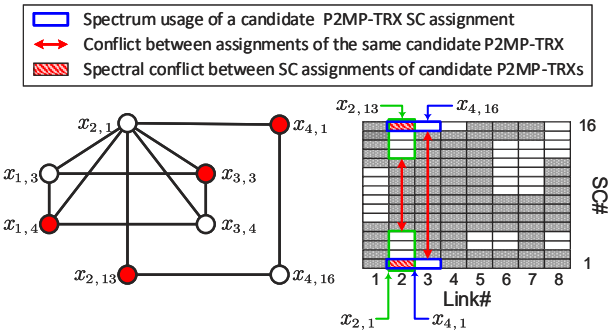

(b) CG-MWIS instance for assigning SCs to leaf P2MP-TRXs.

Fig. 4. An example on the CG-MWIS-based algorithm.

of that in *Algorithm* 1. Hence, in the following, we will focus on the different parts between the two algorithms. In *Line* 4, instead of calculating an LAG based on the availability of the entire k-th FSB, we get the SC availability on links as $\{A_{k,e}, e \in E\}$, where $A_{k,e}$ is a bit-mask denoting the SC availability on link e (*i.e.*, each bit corresponds to an SC within the k-th FSB). Next, we obtain a light-tree $\mathcal{T}_k$ by leveraging $\{A_{k,e}, e \in E\}$ to cover the hub node v and all of its potential leaf nodes in V' (*Line* 5). Specifically, the light-tree is calculated based on weighted link lengths:

$$L'_e = L_e \cdot \left(2 - \frac{\vee[A_{k,e}]}{\hat{S}_o}\right), \tag{31}$$

where L_e is the physical length of a link $e \in E$, and $\hat{S}_o$ is the maximum number of SCs that any type of P2MP-TRX in $O_h \cup O_l$ can use. *Lines* 7-10 find all the feasible SC assignments of candidate leaf P2MP-TRXs based on $\mathcal{T}_k$ and $\{A_{k,e}, e \in E\}$, and store them in set X_k. Then, we use the CG-MWIS-based approach to select SC assignments from X_k, and the results are stored in Y_k (*Lines* 11-13). The remaining part of *Algorithm* 2 is similar to that of *Algorithm* 1.

Complexity analysis: The overall time complexity of *Algorithm* 2 is $O(N_f \cdot (\mathcal{D} + |O_h|) \cdot (|E| + |V|^2 + \hat{S}_o \cdot |V| \cdot \log_{\rho_1}(\rho_2 \cdot \hat{S}_o \cdot |V|)))$ if SPT is used, and $O(N_f \cdot (\mathcal{D} + |O_h|) \cdot (|E| + \hat{S}_o \cdot |V|^2 + \hat{S}_o \cdot |V| \cdot \log_{\rho_1}(\rho_2 \cdot \hat{S}_o \cdot |V|)))$ when MST is applied, where ρ_1 and ρ_2 are the parameters of DistGreedy algorithm [47] to balance its approximation ratio and time complexity.

Algorithm 2: CG-MWIS-based Network Planning

Input: Physical topology $G(V, E)$, traffic demands $\mathbf{D}$.
Output: Overall network planning scheme $\mathbb{Y}$.

```
1  while there are non-zero element(s) in D do
2      select hub node v that maximizes sum_{u in V} D_{v,u};
3      for each k in [1, N_f - F̂_o + 1] do
4          get available SCs on links {A_{k,e}, e in E} to
           deploy a hub P2MP-TRX on v with the k-th FSB;
5          compute a light-tree T_k with {A_{k,e}} to cover v
           and nodes in V' := {u : D_{v,u} > 0, u in V};
6          choose a proper P2MP-TRX o_h in O_h for hub v;
7          for each potential leaf node u in V' do
8              obtain the set of candidate P2MP-TRXs on u
               and find all the feasible SC assignments
               within the k-th FSB for them;
9              insert all the feasible SC assignments of
               candidate P2MP-TRXs in set X_k;
10         end
11         construct a CG G^C(V^C, E^C) based on X_k;
12         find MWIS in the CG with DistGreedy [47];
13         leverage the MWIS to select SC assignments of
           candidate P2MP-TRXs and store them in Y_k;
14         get the number of SCs used on hub P2MP-TRX
           o_h (namely, Z_k) according to Y_k;
15         if Z_k > Z_{k_0} then
16             k_0 = k;
17         end
18     end
19     insert Y_{k_0} in 𝕐 as provisioning scheme of current
       group led by a hub P2MP-TRX on node v;
20     update G(V, E) and D according to Y_{k_0};
21 end
22 Determine the deployment of optical switches and the
   activation of fiber links according to 𝕐;
```

VI. Performance Evaluations

In this section, we conduct numerical simulations to evaluate the performance of the algorithms designed in this work.

A. Simulation Setup

Our simulations consider three physical topologies: 1) the 6-node topology in Fig. 3(a), 2) a 40-node metro topology based on the city of Atlanta, GA [21], and 3) the 14-node Germany topology [48], to investigate the potential of deploying P2MP-TRXs in different network segments (*i.e.*, metro-aggregation, metro and core, respectively). While our proposals can be applied to WSONs with different spectrum allocation granularities, we assume that the WSON is based on the flexible-grid with each FS at $B_f = 12.5$ GHz, and thus each fiber link can accommodate $N_f = 358$ FS' with C-band [27]. To highlight the potential advantages brought by deploying P2MP-TRXs in WSONs, we also consider the scenarios of 1) planning FONs with P2MP-TRXs, and 2) planning WSONs with P2P-TRXs. Specifically, we refer to the optimization models in [19, 20] to modify our LAG-based and CG-based heuristics and make them support the two simulation scenarios, respectively.

In each simulation, we randomly generate traffic demands in $\mathbf{D}$ according to a total traffic amount. Specifically, for each demand, the source and destination are randomly selected, and its bandwidth requirement is chosen within $[10, 100]$ Gbps. Then, we aggregate the generated demands to obtain $\mathbf{D}$. We considered transceiver rates of $\{25, 100, 400\}$ Gbps

TABLE III
SIMULATION RESULTS WITH 6-NODE TOPOLOGY

Total Traffic (Gbps)	ILP Model		LAG-FA			CG-ILP			CG-MWIS		
	Obj.	*Time (s)*	*Obj.*	*Gap*	*Time (s)*	*Obj.*	*Gap*	*Time (s)*	*Obj.*	*Gap*	*Time (s)*
300	2.1389	107,670	2.4027	12.3%	0.0033	2.4132	12.8%	0.0908	2.4193	13.1%	0.0599
600	2.3194	172,800	2.5295	9.06%	0.0046	2.5208	8.68%	0.1895	2.5116	8.28%	0.1047
900	2.3356	172,800	2.5370	8.62%	0.0055	2.4456	4.71%	0.3264	2.5092	7.43%	0.1769
1,200	2.3598	172,800	2.4635	4.40%	0.0324	2.4531	3.95%	0.4662	2.5012	5.99%	0.2181
1,500	2.4209	172,800	2.5653	5.97%	0.0457	2.5431	5.05%	0.8332	2.5591	5.71%	0.2598

for both P2P-TRXs and P2MP-TRXs, while the capacity of 25 Gbps can only be used by leaf P2MP-TRXs or P2P-TRXs [19]. For a P2MP-TRX at $\{25, 100, 400\}$ Gbps, its maximum spectrum usage is $\{1, 2, 6\}$ FS', respectively, and it provides/uses $\{1, 4, 16\}$ SCs, each of which occupies $B_s = 4$ GHz, while the FS usages of P2P-TRXs are proportional to their rates. We assume that $N_g = 1$ FS is reserved as the guard-band on each side of the spectrum assignment of a P2MP-TRX group or a P2P-TRX pair. DP-16QAM is adopted if the length of a lightpath is within 500 km, and dual-polarization quadrature phase shift keying (DP-QPSK) is used otherwise [15]. Then, the capacity of an SC is 25 Gbps and 12.5 Gbps with DP-16QAM and DP-QPSK, respectively. We adopt the cost model in [20] to set the cost of a 25-/100-Gbps P2P-TRX as $\frac{1}{4}/\frac{1}{2}$ of that of a 400-Gbps P2P-TRX, and the costs of P2MP-TRXs in line with those of P2P-TRXs. The price of an optical switch is assumed to be 10 times of that of a 400G P2MP-TRX, and the leasing price of a fiber link is set according to the number of its spans [44], which is estimated based on its physical length [49]. The costs above and the weights in Eq. (1) can be flexibly adjusted. The simulations run on Ubuntu servers with 2.1 GHz Intel Xeon Silver 4110 CPU and 32 GB memory, and the software environment is Python 3.10.2 with Gurobi Optimizer 9.5.2 [50]. To ensure the statistical accuracy of results, we obtain each data point by averaging the results from 10 independent runs.

B. Small-Scale Simulations

We first perform small-scale simulations with the 6-node topology, and set the total amount of traffic demands in $\mathbf{D}$ within $[300, 1500]$ Gbps. Here, we set $\gamma_1 = \gamma_2 = \gamma_3 = \gamma_4 = 1$ and the upper-limit of the ILP's running time as 48 hours (*i.e.*, $172,800$ seconds), and thus, if the ILP cannot obtain the optimal solution after 48 hours, we just select the best-known solution from it. The simulations consider three heuristics, and in addition to LAG-FA and CG-MWIS in *Algorithms* 1 and 2, respectively, we also consider CG-ILP, which generally follows the procedure of *Algorithm* 2, except for solving the ILP in Section V-B directly to get the MWIS in each CG.

Table III summarizes the performance of the algorithms in terms of optimization objective and running time. It can be seen that the ILP always minimizes the normalized CAPEX of a planned WSON the best among all the algorithms, while its running time is also the longest. Specifically, the running time of the ILP reaches its upper-limit when the total traffic is 600 Gbps. CG-ILP performs the best among the heuristics in terms of the objective, but its running time is also the longest among them. LAG-FA outperforms CG-MWIS in most cases, and its running time is also shorter. Meanwhile, it is worth noting that the optimality gaps of the heuristics tend to decrease with the total traffic demand. This is because when the total traffic demand is relatively high, it would be difficult for the ILP solver to find the exact solution within a reasonable period of time and thus it can only return the best-known solution. As the ILP's solution might not be exact anymore, the gap between it and the solution from a heuristic can decrease. Besides, we can see that the optimality gaps of the heuristics, especially CG-MWIS, can fluctuate. On one hand, this is because the heuristics use different resource allocation strategies whose performance towards different network planning instances can vary. On the other hand, certain heuristic (*i.e.*, CG-MWIS) are non-deterministic as randomness has been added into it.

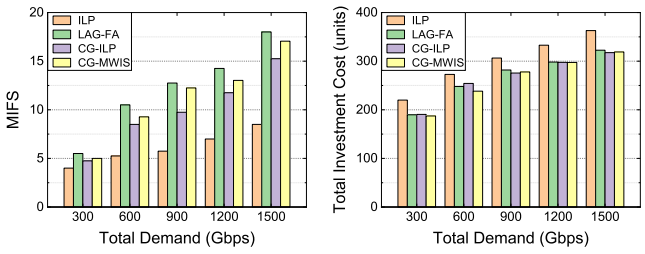

(a) MIFS (b) Total investment cost

Fig. 5. Results of proposed algorithms with 6-node topology.

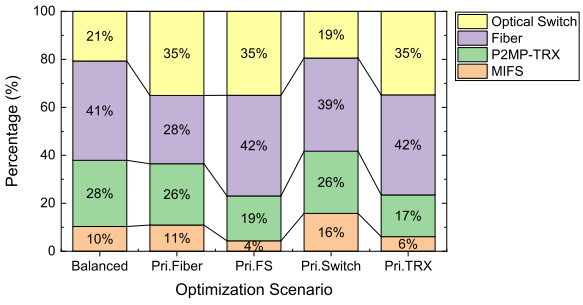

Fig. 6. Simulation results of ILP with different optimization focuses.

Fig. 5 shows the breakdowns of the objective in Eq. (1) in terms of spectrum usage and total investment cost of P2MP-TRXs, optical switches and fiber links. The results on MIFS in Fig. 5(a) suggest that the coarse-grained spectrum assignment in LAG-FA leads to the largest spectrum usage, but Fig. 5(b) shows that LAG-FA can achieve smaller costs of P2MP-TRXs than CG-MWIS in most cases, especially when the traffic amount is relatively large. Finally, we run more simulations

with the ILP to test its adaptability towards different optimization focuses. Specifically, four more scenarios are considered, each of which prioritizes one of the cost components in Eq. (1). This is achieved by making the value of the corresponding weight coefficient much larger than the others. We observe in Fig. 6 that the ILP's solution changes as expected, proving that the ILP can satisfy different importance among the considered cost components by adjusting the relative values of γ_1, γ_2, γ_3 and γ_4. Note that, if the provided resources cannot satisfy all the traffic demands, the network planning will fail [51].

C. Large-Scale Simulations

Large-scale simulations are then performed with the 40-node metro and 14-node Germany topologies to evaluate the proposed heuristics for larger network planning instances. We first compare the P2MP-TRXs and spectra used by different solutions in Figs. 7 and 8, respectively. It can be seen that for the planned WSONs, the P2MP-TRX-based solutions have significantly lower investment costs and spectrum usages in both topologies than their P2P-TRX-based counterparts. This observation conforms to the conclusions in [19, 20] and verifies the benefits of P2MP-TRXs for optical network planning. The planned FONs based on P2MP-TRXs require significantly less CAPEX to satisfy a same set of traffic demands than their WSON counterparts, which confirms the inherent advantage of FON in cost-saving [22]. However, the FONs planned with P2MP-TRXs are only feasible when the total traffic is 15 Tbps or less, and they cannot be planned due to insufficient spectrum resources, otherwise. The higher spectrum efficiency in WSONs is achieved at the expense of additional cost of optical switches, and thus WSON will become a necessary choice when we need to architect an optical network with P2MP-TRXs to adapt to a large volume of traffic demands.

As for our heuristics for planning WSONs with P2MP-TRXs, CG-ILP outperforms LAG-FA and CG-MWIS in terms of spectral usage in the metro topology (in Fig. 8(a)), while LAG-FA is the most spectral-efficient in the Germany topology, especially for relatively high traffic loads (in Fig. 8(b)). The heuristics perform similarly on P2MP-TRX cost for low traffic loads in both topologies, but LAG-FA gives the lowest P2MP-TRX cost when the traffic load is relatively high (in Fig. 7). These results suggest that in the WSONs that are physically larger and carry high traffic loads, sophisticated spectrum allocation would be more effective than only focusing on avoiding spectrum fragmentation. CG-MWIS provides similar spectrum usages as CG-ILP by virtue of the adopted approximation algorithm (*i.e.*, DistGreedy), but its performance on P2MP-TRX cost can be worse, suggesting that DistGreedy can sometimes deploy leaf P2MP-TRXs in sub-optimal manners.

Fig. 9 shows the spectral fragmentation and overall spectral usage of the WSONs planned by the heuristics. Here, we adopt the Shannon entropy-based metrics [52] to measure spectrum fragmentation. It can be seen that with fine-grained spectrum assignment, CG-ILP and CG-MWIS can achieve noticeable reduction on spectrum fragmentation over LAG-FA. Specifically, the coarse-grained spectrum assignment scheme in LAG-FA can fragment the spectra in a WSON more as

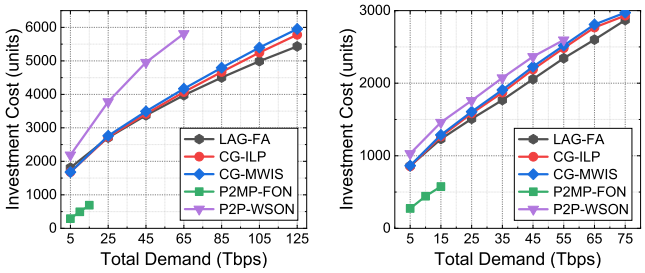

(a) 40-node metro topology (b) 14-node Germany topology

Fig. 7. Total investment cost of the WSONs planned by the heuristics.

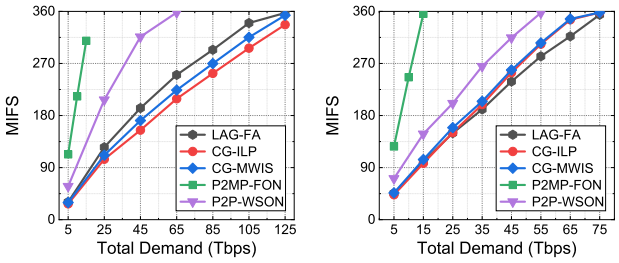

(a) 40-node metro topology (b) 14-node Germany topology

Fig. 8. MIFS of used FS'of the WSONs planned by the heuristics.

more traffic demands are served, which can make it difficult for future demands to use the remaining spectra. Moreover, the results in Fig. 9 also show that CG-ILP and CG-MWIS can utilize the spectra in a WSON more efficiently than LAG-FA.

Finally, we compare the running time of the heuristics in Fig. 10. We observe that LAG-FA only needs roughly one sixth of the running time of CG-MWIS, which makes it the most time-efficient algorithm among the three heuristics. The excellent performance of CG-ILP in spectrum utilization is achieved at the cost of longest running time (*i.e.*, significantly longer than the running time of LAG-FA), as ILP instances for SC assignments have to be formulated and solved repeatedly, so as to find the currently best deployment scheme that can efficiently utilize fragmented spectra in the WSON.

VII. Conclusion

In this paper, we studied the network planning of WSONs with DSCM-enabled P2MP-TRXs, aiming to minimize the CAPEX of planned networks. An ILP model was formulated to formally describe the problem and solve it exactly. Then, we proposed two heuristics, namely, LAG-FA and CG-MWIS, to find near-optimal solutions in polynomial time. In LAG-FA, LAGs were built to compute light-trees and two fragmentation-related metrics were designed to prioritize the deployment of P2MP-TRXs and their SC assignments. As for CG-MWIS, fine-grained search of available spectrum was achieved by a CG-based approach to better utilize the available yet fragmented spectrum, and then the problem of SC assignment was solved by finding the MWIS in the CG. Finally, extensive simulations were performed to evaluate the proposed algorithms, and the benefits of CG-MWIS over LAG-FA were confirmed by the results.

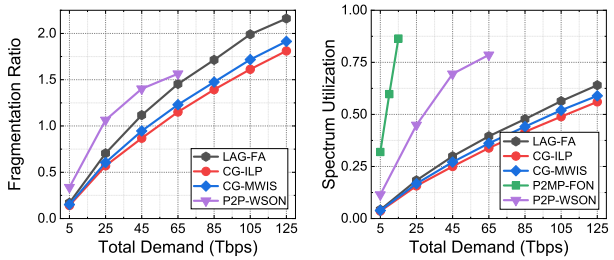

(a) 40-node metro topology

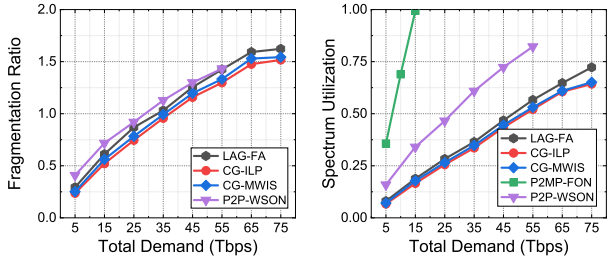

(b) 14-node Germany topology

Fig. 9. Fragmentation ratio and spectrum utilization.

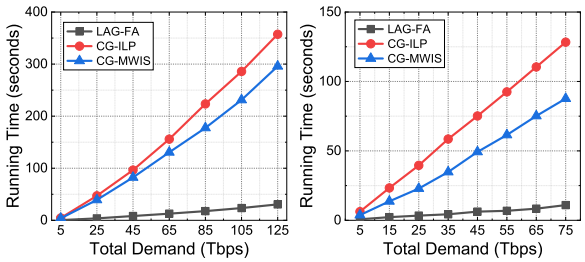

(a) 40-node metro topology (b) 14-node Germany topology

Fig. 10. Running time of the proposed heuristics.

ACKNOWLEDGMENTS

This work was supported by the NSFC project 62371432.

REFERENCES

[1] "Cisco Annual Internet Report (2018-2023)." [Online]. Available: https://www.cisco.com/c/en/us/solutions/collateral/executive-perspectives/annual-internet-report/white-papper-c11-741490.html.

[2] J. Liu *et al.*, "On dynamic service function chain deployment and readjustment," *IEEE Trans. Netw. Serv. Manag.*, vol. 14, pp. 543–553, Sept. 2017.

[3] P. Lu *et al.*, "Highly-efficient data migration and backup for Big Data applications in elastic optical inter-datacenter networks," *IEEE Netw.*, vol. 29, pp. 36–42, Sept./Oct. 2015.

[4] Z. Zhu, W. Lu, L. Zhang, and N. Ansari, "Dynamic service provisioning in elastic optical networks with hybrid single-/multi-path routing," *J. Lightw. Technol.*, vol. 31, pp. 15–22, Jan. 2013.

[5] W. Shi, Z. Zhu, M. Zhang, and N. Ansari, "On the effect of bandwidth fragmentation on blocking probability in elastic optical networks," *IEEE Trans. Commun.*, vol. 61, pp. 2970–2978, Jul. 2013.

[6] Y. Yin *et al.*, "Spectral and spatial 2D fragmentation-aware routing and spectrum assignment algorithms in elastic optical networks," *J. Opt. Commun. Netw.*, vol. 5, pp. A100–A106, Oct. 2013.

[7] C. Chen *et al.*, "Demonstrations of efficient online spectrum defragmentation in software-defined elastic optical networks," *J. Lightw. Technol.*, vol. 32, pp. 4701–4711, Dec. 2014.

[8] K. Wu, P. Lu, and Z. Zhu, "Distributed online scheduling and routing of multicast-oriented tasks for profit-driven cloud computing," *IEEE Commun. Lett.*, vol. 20, pp. 684–687, Apr. 2016.

[9] S. Li, D. Hu, W. Fang, and Z. Zhu, "Source routing with protocol-oblivious forwarding (POF) to enable efficient e-health data transfers," in *Proc. of ICC 2016*, pp. 1–6, Jun. 2016.

[10] M. Ju, F. Zhou, S. Xiao, and Z. Zhu, "Power-efficient protection with directed p-cycles for asymmetric traffic in elastic optical networks," *J. Lightw. Technol.*, vol. 34, pp. 4053–4065, Sept. 2016.

[11] M. Jinno *et al.*, "Multiflow optical transponder for efficient multilayer optical networking," *IEEE Commun. Mag.*, vol. 50, pp. 56–65, May 2012.

[12] D. Welch *et al.*, "Point-to-multipoint optical networks using coherent digital subcarriers," *J. Lightw. Technol.*, vol. 39, pp. 5232–5247, Aug. 2021.

[13] M. Hadi and E. Agrell, "Joint power-efficient traffic shaping and service provisioning for metro elastic optical networks," *J. Opt. Commun. Netw.*, vol. 11, pp. 578–587, Dec. 2019.

[14] D. Welch *et al.*, "Digital subcarriers: A universal technology for next generation optical networks," in *Proc. of OFC 2022*, pp. 1–3, Mar. 2022.

[15] M. Hosseini *et al.*, "Long-term cost-effectiveness of metro networks exploiting point-to-multipoint transceivers," in *Proc. of ONDM 2022*, pp. 1–6, May 2022.

[16] J. Back *et al.*, "CAPEX savings enabled by point-to-multipoint coherent pluggable optics using digital subcarrier multiplexing in metro aggregation networks," in *Proc. of ECOC 2020*, pp. 1–4, Dec. 2020.

[17] M. Hosseini *et al.*, "Optimized design of metro-aggregation networks exploiting digital subcarrier routing," in *Proc. of ACP 2021*, pp. 1–3, Oct. 2021.

[18] J. Back *et al.*, "A filterless design with point-to-multipoint transceivers for cost-effective and challenging metro/regional aggregation topologies," in *Proc. of ONDM 2022*, pp. 1–6, May 2022.

[19] P. Pavon-Marino *et al.*, "On the benefits of point-to-multipoint coherent optics for multilayer capacity planning in ring networks with varying traffic profiles," *J. Opt. Commun. Netw.*, vol. 14, pp. B30–B44, May 2022.

[20] M. Hosseini *et al.*, "Optimization of survivable filterless optical networks exploiting digital subcarrier multiplexing," *J. Opt. Commun. Netw.*, vol. 14, pp. 586–594, Jul. 2022.

[21] C. Tremblay *et al.*, "Agile metropolitan filterless optical networking," in *Proc. of FNWF 2022*, pp. 113–116, Oct. 2022.

[22] O. Ayoub *et al.*, "Tutorial on filterless optical networks," *J. Opt. Commun. Netw.*, vol. 14, pp. 1–15, Mar. 2022.

[23] Z. Zhu *et al.*, "RF photonics signal processing in subcarrier multiplexed optical-label switching communication systems," *J. Lightw. Technol.*, vol. 21, pp. 3155–3166, Dec. 2003.

[24] Y. Zhang, M. O'Sullivan, and R. Hui, "Digital subcarrier multiplexing for flexible spectral allocation in optical transport network," *Opt. Express*, vol. 19, pp. 21 880–21 889, Oct. 2011.

[25] L. Velasco *et al.*, "Autonomous and energy efficient lightpath operation based on digital subcarrier multiplexing," *IEEE J. Sel. Areas Commun.*, vol. 39, pp. 2864–2877, Sept. 2021.

[26] D. Welch *et al.*, "Digital subcarrier multiplexing: Enabling software-configurable optical networks," *J. Lightw. Technol.*, vol. 41, pp. 1175–1191, Feb. 2023.

[27] L. Gong, X. Zhou, W. Lu, and Z. Zhu, "A two-population based evolutionary approach for optimizing routing, modulation and spectrum assignments (RMSA) in O-OFDM networks," *IEEE Commun. Lett.*, vol. 16, pp. 1520–1523, Sept. 2012.

[28] L. Gong *et al.*, "Efficient resource allocation for all-optical multicasting over spectrum-sliced elastic optical networks," *J. Opt. Commun. Netw.*, vol. 5, pp. 836–847, Aug. 2013.

[29] X. Liu, L. Gong, and Z. Zhu, "On the spectrum-efficient overlay multicast in elastic optical networks built with multicast-incapable switches," *IEEE Commun. Lett.*, vol. 17, pp. 1860–1863, Sept. 2013.

[30] Z. Zhu *et al.*, "Impairment- and splitting-aware cloud-ready multicast provisioning in elastic optical networks," *IEEE/ACM Trans. Netw.*, vol. 25, pp. 1220–1234, Apr. 2017.

[31] H. Sun *et al.*, "800G DSP ASIC design using probabilistic shaping and digital sub-carrier multiplexing," *J. Lightw. Technol.*, vol. 38, pp. 4744–4756, Sept. 2020.

[32] "The ultimate guide to nyquist subcarriers." [Online]. Available: https://www.infinera.com/wp-content/uploads/The-Ultimate-Guide-to-Nyquist-Subcarriers-0208-WP-RevA-0719.pdf.

[33] A. Rashidinejad *et al.*, "Real-time demonstration of 2.4Tbps (200Gbps/λ) bidirectional coherent DWDM-PON enabled by coherent nyquist subcarriers," in *Proc. of OFC 2020*, pp. 1–3, Mar. 2020.

[34] A. Napoli *et al.*, "Live network demonstration of point-to-multipoint coherent transmission for 5G mobile transport over existing fiber plant," in *Proc. of ECOC 2021*, pp. 1–4, Sept. 2021.

[35] N. Skorin-Kapov, F. Muro, M. Delgado, and P. Pavon-Marino, "Point-to-multipoint coherent optics for re-thinking the optical transport: Case

study in 5G optical metro networks," in *Proc. of ONDM 2021*, pp. 1–4, Jun. 2021.
[36] D. Moniz, V. Lopez, and J. Pedro, "Design strategies exploiting C+L-band in networks with geographically-dependent fiber upgrade expenditures," in *Proc. of OFC 2020*, pp. 1–3, Mar. 2020.
[37] Y. Ma *et al.*, "Recent progress of wavelength selective switch," *J. Lightw. Technol.*, vol. 39, pp. 896–903, Feb. 2021.
[38] "Finisar. Single Wavelength Selective Switch (WSS)." [Online]. Available: https://finisarwss.com/wp-content/uploads/2020/07/FinisarWSS_Single_Wavelength_Selective_Switch_ProductBrief_Jun2020.pdf.
[39] "Open XR Forum." [Online]. Available: https://www.openxrforum.org/.
[40] A. Gumaste, J. Pedro, and H. Bock, "Exploring point-to-multipoint coherent capabilities across metro and core networks," in *Proc. of ECOC 2022*, pp. 1–4, Sept. 2022.
[41] K. Christodoulopoulos, I. Tomkos, and E. Varvarigos, "Elastic bandwidth allocation in flexible OFDM-based optical networks," *J. Lightw. Technol.*, vol. 29, pp. 1354–1366, May 2011.
[42] X. Liu, L. Gong, and Z. Zhu, "Design integrated RSA for multicast in elastic optical networks with a layered approache," in *Proc. of GLOBECOM 2013*, pp. 2346–2351, Dec. 2013.
[43] L. Gong and Z. Zhu, "Virtual optical network embedding (VONE) over elastic optical networks," *J. Lightw. Technol.*, vol. 32, pp. 450–460, Feb. 2014.
[44] V. Dukic *et al.*, "Beyond the mega-data center: Networking multi-data center regions," in *Proc. of ACM SIGCOMM 2020*, pp. 765–781, Aug. 2020.
[45] M. Fredman and R. Tarjan, "Fibonacci heaps and their uses in improved network optimization algorithms," *J. ACM*, vol. 34, pp. 596–615, Jul. 1987.
[46] L. Kou, G. Markowsky, and L. Berman, "A fast algorithm for Steiner trees," *Acta Inform.*, vol. 15, pp. 141–145, Jun. 1981.
[47] C. Joo, X. Lin, J. Ryu, and N. Shroff, "Distributed greedy approximation to maximum weighted independent set for scheduling with fading channels," *IEEE/ACM Trans. Netw.*, vol. 24, pp. 1476–1488, Jun. 2016.
[48] J. Pedro, N. Costa, and S. Sanders, "Cost-effective strategies to scale the capacity of regional optical transport networks," *J. Opt. Commun. Netw.*, vol. 14, pp. A154–A165, Feb. 2022.
[49] S. Korotky, "Price-points for components of multi-core fiber communication systems in backbone optical networks," *J. Opt. Commun. Netw.*, vol. 4, no. 5, pp. 426–435, 2012.
[50] "Gurobi Optimizer Reference Manual." [Online]. Available: https://www.gurobi.com.
[51] J. Pedro, N. Costa, and S. Sanders, "Scaling regional optical transport networks with pluggable and integrated high-capacity line interfaces," in *Proc. of OFC 2021*, pp. 1–3, Jun. 2021.
[52] P. Wright, M. Parker, and A. Lord, "Minimum- and maximum-entropy routing and spectrum assignment for flexgrid elastic optical networking," *J. Opt. Commun. Netw.*, vol. 7, pp. A66–A72, Jan. 2015.